Optical birefringence data on the phase transitions in $Rb_{1-x}(NH_4)_xH_2AsO_4$

1993 J. Phys.: Condens. Matter 5 1133

(http://iopscience.iop.org/0953-8984/5/8/014)

J. Phys.: Condens. Matter 5 (1993) 1133–1138. Printed in the UK

Optical birefringence data on the phase transitions in $Rb_{1-x}(NH_4)_xH_2AsO_4$

V Westphal†, W Kleemann† and Sook-Il Kwun‡

† Angewandte Physik, Universität Duisburg, W-4100 Duisburg 1, Federal Republic of Germany

‡ Department of Physics, Seoul National University, Seoul, Korea

Received 25 September 1992, in final form 27 November 1992

Abstract. Based on measurements of spontaneous linear birefringence, the phase diagram of $Rb_{1-x}(NH_4)_xH_2AsO_4$ has been completed. The ferroelectric compounds ($x < 0.19$) undergo second-order transitions, whereas the antiferroelectric transitions ($x > 0.46$) are strongly first-order.

1. Introduction

The competing interaction system $Rb_{1-x}(NH_4)_xH_2PO_4$ (RADP) has attracted considerable attention in recent years [1] because of its remarkable resemblance to analogous spin systems. It undergoes transitions into structural glass phases at intermediate concentrations, $0.22 \leqslant x \leqslant 0.74$, whereas ferroelectric (FE) ($x < 0.22$) and antiferroelectric AFE ($x > 0.74$) phase transitions (PT) occur when approaching the marginal compounds of the system. These are characterized by nearly equal PT temperatures, $T_c = 146$ K (RbH_2PO_4, RDP for short) and $T_N = 147$ K ($NH_4H_2PO_4$, ADP), and hence, nearly equal ferro- and antiferroelectric interactions, respectively. In contrast, the related system $Rb_{1-x}(NH_4)_xH_2AsO_4$ (RADA) involves marginal compounds with strongly different PT temperatures, $T_c = 110$ K for RbH_2AsO_4 (RDA) and $T_N = 216$ K for $NH_4H_2AsO_4$ (ADA) [2]. That is why the phase diagram, PT temperature T versus x, appears more symmetric for RADA [3] than for RADP. The intermediate glassy regime extends over the approximate concentration range $0.15 < x < 0.45$ [4].

In the present paper we complete the x–T phase diagram of RADA [4] by novel linear birefringence (LB) data, which have proved to yield quite reliable results for both the RADP [1] and the RADA system [5]. We attempt to describe the phase diagram within a cluster approximation [6] taking into account the large difference in PT temperatures, $T_N(\text{ADA}) \simeq 2T_c(\text{RDA})$. However, owing to the simplicity of the theoretical approach the agreement with the experimental data is unsatisfactory.

A non-classical near-critical exponent $\beta \simeq 0.59$ is observed for FE RADA with various concentrations $0.13 \leqslant x \leqslant 0.19$. Presumably the deviation from the expected mean-field critical value $\beta = 0.5$ is due to temperature-dependent Landau expansion parameters as found for pure RDP [7].

0953-8984/93/081133+06$07.50

2. Experimental details

Mixed crystals of RADA were grown from aqueous solutions, cut and polished to yield optically transparent platelets with thickness $d \simeq 1$ mm and surfaces oriented parallel to (010) and (001), respectively [4]. The corresponding LB, Δn_{ac} and Δn_{ab}, was measured [8] with a resolution of better than $\delta \Delta n \simeq 10^{-6}$ at a light wavelength $\lambda = 589.3$ nm on microscopically selected sample areas, $A \simeq 10^{-10}$ m^2, with uniform orientation and thickness in the temperature range $7 \leqslant T \leqslant 300$ K stabilized to within $\delta T \simeq 0.05$ K.

3. Experimental results and discussion

The Curie and Néel temperatures of various mixtures of RADA, $x = 0.8$, 0.13, 0.17, 0.19, 0.20, 0.37, 0.49 and 0.70, have been determined by inspecting the temperature dependence of the morphic LB within the a–b plane of well-oriented single-crystal samples [5]. By use of a polarizing microscope, well defined orthorhombic low-T single domains were selected in order to exploit the connection with the spontaneous polarization, P_3 [1]

$$\Delta n_{12} = n_0^3 \rho_{63} P_3 \tag{1}$$

in case of a FE PT, where the optical polarization coefficient ρ_{63} is assumed to account for ferroelastic contributions, as well [9]. n_0 is the average unperturbed refractive index. Figure 1 shows some of the LB curves at temperatures $0.8 \leqslant T/T_c \leqslant 1.2$, where $T_c = 85.3$, 78.4 and 70.8 K for $x = 0.13$, 0.17 and 0.19, respectively.

Fits of the data in figure 1 to a power law

$$P_3(T) = P_3^0(1 - T/T_c)^\beta \tag{2}$$

within the range $0.95 \leqslant T/T_c \leqslant 0.98$ reveal an exponent $\beta = 0.59 \pm 0.01$ for all three concentrations. We excluded values closer to T_c than those given by the condition $1 - T/T_c < 2 \times 10^{-2}$, because of obvious smearing due to concentration gradients. Therefore, the above exponent constitutes an effective value, which significantly deviates from the expected mean-field one, $\beta = 0.5$. Unfortunately the critical behaviour of P_3 in pure RDA is unknown. Since the RADA value, $\beta = 0.59$, seems to be independent of x, the same value is conjectured to apply to RDA, as well. If so, its deviation from $\beta = 0.5$ might be explained by relevant temperature dependence of the quartic Landau expansion coefficient as introduced by Trussaut and Vallade [7] in the case of pure RDP and, more generally, for structural phase transitions outside the Ginzburg region by Heine *et al* [10].

The PT of pure ADA at $T_N = 216$ K is strongly discontinuous. Correspondingly, the morphic LB within the a–b plane exhibits a strong jump, although, to the best of our knowledge, this has never been observed experimentally in either ADP and ADA. The reason lies in the extremely large lattice deformation in the AFE phase leading to shattering of the initial single-crystal sample [2].

In the case of 'diluted' ADA, $x = 0.7$, we have succeeded in selecting small structural single domains, although the samples as a whole are generally destroyed after undergoing the PT. Figures 2 and 3 show the morphic and natural LB

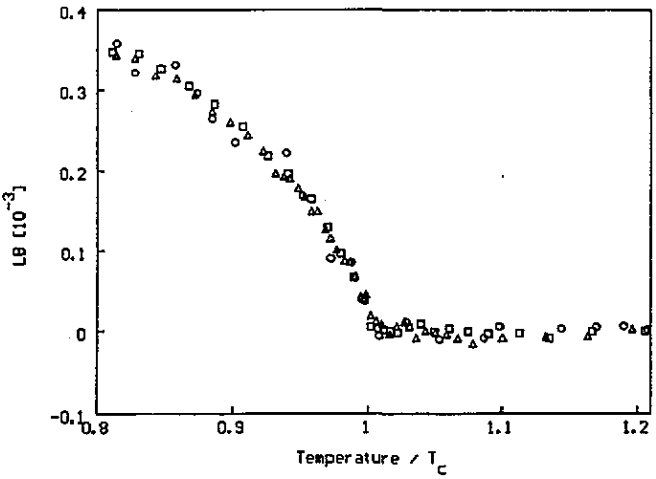

Figure 1. Linear birefringence Δn_{12} versus T/T_c of RADA with $x = 0.13$ (□, $T_c = 85.3$ K), 0.17 (△, $T_c = 78.4$ K) and 0.19 (○, $T_c = 70.8$ K).

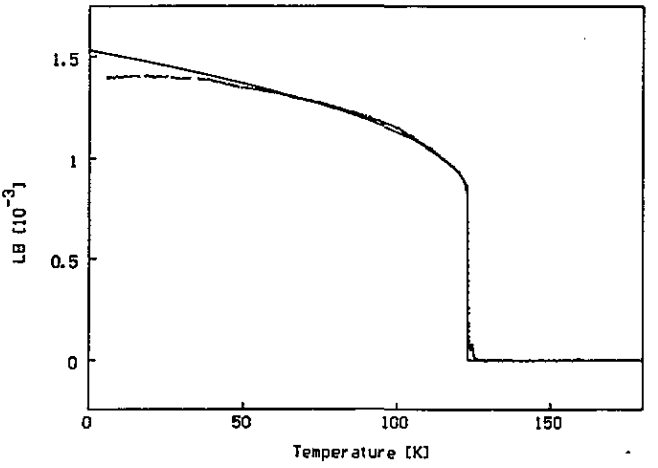

Figure 2. Linear birefringence Δn_{12} versus T of RADA with $x = 0.70$ (data points) fitted to a Landau type theoretical curve (solid line, see text).

curves, Δn_{12} and $\Delta n_{31,32}$, respectively. Both of them experience discontinuities at $T_N = 123.4$ K, $\delta\Delta n = 0.9$ and 4.0×10^{-3}, respectively, which are proportional to the intraplanar spontaneous strain, $e_{2s} - e_{1s}$. The large difference between both Δn jumps is very probably due to large differences in the elasto–optic coefficients involved, $p_{11} - p_{12}$ and $p_{11} - p_{13,23}$, respectively. The thermo–optic background of $\Delta n_{31,32}$ is subtracted in figure 3 by using a Debye function as in our previous paper [5] (solid line). The Debye temperature emerging as a best-fit parameter, $\Theta_D = 683$ K, is close to that of AFE RADA with $x = 0.49$, $\Theta_D = 712$ K [5]. The contribution of the PT to $\Delta n_{31,32}$ (lower curve in figure 3) is roughly proportional to the morphic LB, Δn_{12} (figure 2). Note that $\Delta n_{31,32}$ reveals a fluctuation tail at $T > T_N$ as usual for non-morphic LB at a structural PT [8], even in the strongly first-order case [11].

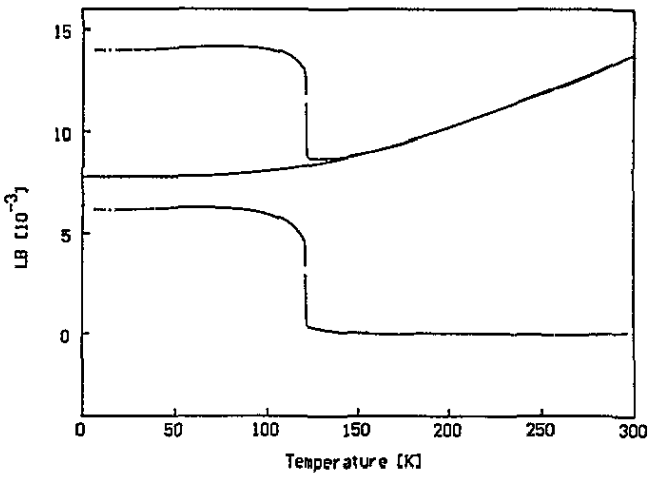

Figure 3. Linear birefringence $\Delta n_{31,32}$ versus T of RADA with $x = 0.70$ (upper curve). After subtraction of the Debye type thermo-optic background (solid line) the antiferroelectric contribution (lower curve) is obtained.

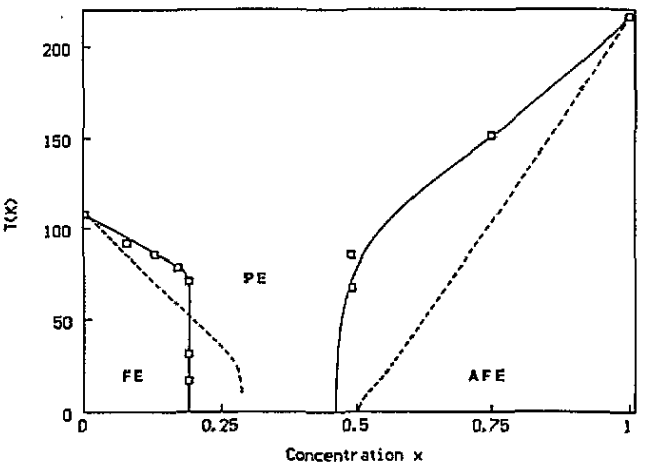

Figure 4. Phase diagram of RADA as measured (data points and interpolated solid lines) and calculated within a cluster-theoretical approach [6] (broken lines). The phases are denoted by FE (ferroelectric), PE (paraelectric) and AFE (antiferroelectric).

We have attempted to fit the morphic LB of RADA with $x = 0.70$ to a Landau theoretical expression which assumes Δn_{12} to be proportional to the square of the AFE order parameter ξ at a first-order PT [11]. Here we assume proportionality between $e_{2s} - e_{1s}$ and ξ^2. The resulting curve, fitted within $122.6 \leqslant T \leqslant 123.4$ K, is shown in figure 2 (solid line). It describes the LB curve pretty well down to $T_N/2$. At $T < 60$ K the typical flattening of the LB due to quantum effects destroys the agreement with the theoretical curve.

LB measurements on RADA with $x = 0.49$ were performed previously [5]. They reveal two successive PT at $T_{N1} = 85$ K and $T_{N2} \simeq 60$ K accompanied by a 45°

rotation of the orthorhombic a and b axes below T_{N2}. Crystallographic details of this unexpected feature are still lacking.

Glassy behaviour of samples with $x = 0.20$ and 0.37 is clearly reflected by the complete absence of morphic birefringence, Δn_{12}, at all temperatures [5]. Spurious effects are occasionally found as a consequence of improper sample alignment. In contrast, the frozen-in short-range order, $\langle P_3^2 \rangle$, gives rise to typical anomalies superimposed on the non-morphic a–c plane LB, $\Delta n_{31.32}$ [5]. Similar anomalies have been observed in the otherwise non-birefringent basal plane of an $x = 0.20$ sample upon application of a moderate electric field along one of the intraplanar a axes. Presumably this effect originates from an induced ferroelectric moment similarly as observed in nearly FE glassy RADP with $x = 0.22$ [12].

All experimental phase boundary data are presented in figure 4. Previous experimental data [4, 5] fit well with the present ones. It is interesting to note that the FE phase boundary drops very steeply at $x_F = 0.19$. In fact, one sample with a nominal concentration $x = 0.19$ happened to reveal both FE ($x < x_F$) and glassy behaviour ($x > x_F$) at different positions selected on the c plane with the polarizing microscope. Within a distance of about 1 mm a state with FE multidomains changed over into an optically homogeneous state at $T < 50$ K. Very probably this hints at spurious concentration gradients in the vicinity of $x = x_F$, as similarly conjectured previously [12] in the case of RADP with $x = 0.22$. Within the FE part of the RADA sample with $x = 0.19$ various PT temperatures between $T_c = 25$ K and 75 K were verifiable on different single-domain areas sized about $(5\ \mu m)^2$.

Comparison of the phase diagram with theoretical predictions is not yet available. In a preliminary study we adapted the cluster theory of Matsushita and Matsubara [6] to the situation of RADA, where $T_N(\text{ADA}) \simeq 2T_c(\text{RDA})$. It is known that the approach of [6] accounts only very crudely for the origin of the antiferroelectric interaction of the ADA component. Hence, we consider it to be a mere phenomenological first approximation, whose mean-field equations have the advantage of being straightforwardly solvable. More exact models like that of Selke and Courtens [13] require extensive Monte Carlo calculations, which are outside the scope of this paper. Figure 4 shows the results of our calculations (dashed lines). We find qualitative agreement of the asymmetry of the phase diagram. Apart from this, however, many features disagree. In particular, the steepness of the phase boundaries near the proton glass gap is unsatisfactorily modelled. Better agreement is expected upon application of more sophisticated theories [13].

4. Conclusion

By using locally resolved LB measurements the x–T phase diagram of RADA has been completed. The proton glass gap extends between $x_F = 0.20$ and $x_A \simeq 0.46$. At these boundaries the FE and AFE phase lines, respectively, drop very sharply towards $T = 0$. Cluster theoretical calculations of the phase diagram [6], adapted to the interaction parameters of RADA, yield only poor agreement.

References

[1] Courtens E 1983 *Helv. Phys. Acta* **56** 705; 1985 *Japan. J. Appl. Phys.* **24** S2, 70

[2] Lines M E and Glass A M 1979 *Principles and Applications of Ferroelectric and Related Materials* (Oxford: Clarendon) p 293f
[3] Trybula Z, Stankowski J, Szczepanska L, Blinc R, Weiss A and Dalal N S 1988 *Physica* B **153** 143
[4] Kim S and Kwun S I 1990 *Phys. Rev.* B **42** 638
[5] Sommer D, Kleemann W, Yoon J G, Kwun S I and Kim S 1990 *Ferroelectrics* **106** 131
[6] Matsushita E and Matsubara T 1984 *Prog. Theor. Phys.* **71** 235
[7] Trussaut F and Vallade M 1980 *J. Phys. C: Solid State Phys.* **13** 4649
[8] Schäfer F J and Kleemann W 1985 *J. Appl. Phys.* **57** 2606
[9] Fousek J and Petzelt J 1979 *Phys. Status Solidi* a **55** 11
[10] Heine V, Chen X, Dattagupta S, Evans A, Giddy A P, Marais S, Padlewski S, Salje E and Tautz F S 1992 *Ferroelectrics* **128** 255
[11] Kleemann W, Schäfer F J and Fontana M D 1984 *Phys. Rev.* B **30** 1148
Kleemann W, Schäfer F J and Rytz D 1986 *Phys. Rev.* B **34** 7873
[12] Amin S 1989 *Z. Phys.* B **74** 113
[13] Selke W and Courtens E 1986 *Ferroelectr. Lett.* **5** 173